

Performance Comparison of Surface and Spoke Type Flux-Modulation Machines with Different Pole Ratios

Tianjie Zou, *Student Member, IEEE*, Dawei Li*, *Member, IEEE*, Ronghai Qu, *Senior Member, IEEE*,
 and Dong Jiang, *Senior Member, IEEE*

State Key Laboratory of Advanced Electromagnetic Engineering and Technology,
 School of Electrical and Electronic Engineering,
 Huazhong University of Science and Technology, Wuhan 430074, China.

In this paper, performance comparison between surface and spoke type flux modulation (FM) PM machines is presented. Generally, spoke-array magnet arrangement is capable of increasing the torque density of PM machines due to its flux focusing effect. Nevertheless, a flux barrier effect is found when this magnet topology is applied in FM machines, which may offset the advantage in torque capability when the pole ratio is high. By flux distribution comparison of these two machine topologies, the flux barrier effect is visually explained. Through numerical FEA, this effect is further investigated in spoke type vernier PM machines with a series of pole ratios. Finally, compared with surface type FM machines, considerable reduction in modulated magnetic field as well as output torque capability is verified in high pole ratio, spoke type FM machines.

Index Terms—Flux barrier, flux modulation, vernier, flux switching, spoke-array, pole ratio.

I. INTRODUCTION

DIRECT-drive permanent magnet (PM) machines have been widely used in recent years. In many applications such as wind power and ship propulsion, PM machines are designed to work at low-speed, high-torque operation mode. However, the high torque demand always leads to a bulky machine size and large material consumption. Therefore, high torque density PM machines are eagerly researched. Many novel PM machine topologies with superior torque density have been proposed, such as transverse flux machines, magnetic geared machines and vernier PM machines. These machine topologies have been found to share the same working principle, i.e., the flux modulation effect, and thus can be classified into the flux-modulation (FM) machine family [1].

According to the position of magnets, PM machines can further be classified into surface type and interior type. The spoke-array magnet disposition, has drawn more and more attentions due to its inherent flux focusing effect [2]. This magnet arrangement has been proven capable of producing higher airgap flux density compared with that of the surface type, while sometimes at the cost of more PM material usage. Meanwhile, apart from the commonly used surface mounted PMs, spoke-array magnet arrangement have also been applied in some of the flux modulation machines to further improve their torque density [3-5].

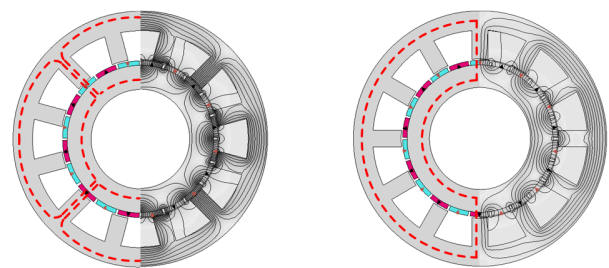
This paper provides the performance comparison of surface and spoke type FM machines. Through flux distribution comparison, a flux barrier effect is found in spoke type FM machines. Based on numerical FEA, this effect is quantitatively analyzed with different machine pole ratios. Due to this effect, considerable reduction in modulated field and torque capability is verified in spoke type FM machines.

II. TYPICAL MACHINE TOPOLOGY AND FLUX DISTRIBUTION

In classic electrical machine theory, the stator and rotor pole pair number should keep the same to achieve electromechanical

energy conversion. Nevertheless, this law is not suitable for FM machines. Due to the existence of flux modulator, two magnetic fields with different pole number and rotating speed, excited by the stator and rotor respectively, can be coupled and produce steady torque. Pole ratio (PR) is a special design parameter for FM machine and defined as the ratio of rotor to stator pole number.

Vernier PM machine can be used as a typical machine topology to illustrate the flux modulation effect. Generally, a regular vernier PM machine is constructed with a surface mounted PM rotor and a stator with large slot opening, as shown in Fig. 1. The magnetomotive force (MMF) developed by PMs can be expressed by (1), where P_r is the PM pole pair number, θ_s the mechanical angle on the stator, ω the electrical angular velocity. The airgap permeance of the open slot-tooth structure is described by (2) instead of the commonly used Carter's coefficient, where Z is the stator slot number.



(a) 12/10 stator slot/rotor pole pair combination. Pole ratio=5:1. (b) 12/11 stator slot/rotor pole pair combination. Pole ratio=11:1.
 Fig. 1. Flux distribution of surface mounted VPM machines.

$$F_c(\theta_s, t) = \sum_{i=1,3,5,\dots} F_{ci} \cos(iP_r\theta_s - i\omega t) \approx F_{c1} \cos(P_r\theta_s - \omega t) \quad (1)$$

$$\Lambda(\theta_s) = \Lambda_0 + \Lambda_Z \cos(Z\theta_s) \quad (2)$$

The airgap flux density B_g is then calculated in (3) by multiplying (1) and (2), where $B_{conv} = F_{c1}\Lambda_0$ and $B_{modu} = 0.5F_{c1}\Lambda_1$. The first term in (3) with pole pair number of P_r is a conventional component which also exist in regular PM

machines. The second term in (3) is an additional part, which is produced through the flux modulation effect. The pole pair number of the stator winding P_s is then designed according to (4), which makes B_{conv} and B_{modu} slot harmonics of each other. In this paper, $P_r=Z-P_s$ is chosen for further discussion, since this combination has been proved to own higher torque density. According to [1], the average electromagnetic torque is directly given by (5), where k_ω is the winding factor, N_s the turns in series per phase, I the RMS value of phase current, r_g the airgap radius and L the stack length.

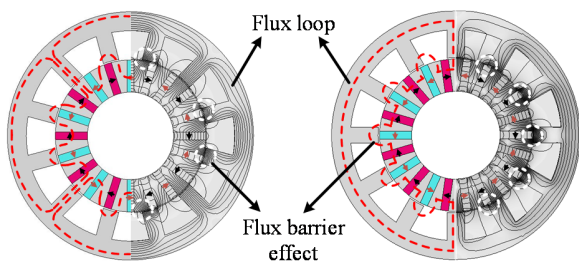
As vernier PM machine is equipped with relatively large and close slot and rotor pole pair numbers, P_s is always much smaller than P_r . As can be seen from (5), the contribution of B_{modu} is amplified by the pole ratio in torque production. Essentially, it is exactly this additional modulated component that makes vernier machine an inherently high torque density machine topology. Therefore, it is an important criteria in VPM machine design to obtain considerable amplitude of modulated magnetic field with a small pole pair number of P_s .

$$B_g = B_{conv}(\cos P_r \theta_s + \omega t) + B_{modu} \{ [\cos(Z - P_r) \theta_s + \omega t] + [\cos(Z + P_r) \theta_s - \omega t] \} \quad (3)$$

$$P_s = |Z - P_r| \quad (4)$$

$$T_e = 3\sqrt{2}k_\omega N_s I (r_g L) (B_{conv} + \frac{P_r}{P_s} B_{modu}) \quad (5)$$

Fig. 1(a) and (b) illustrate the no load flux distribution of two surface mounted VPM machines, with $P_s=2$ and 1, respectively. Since P_s is much smaller than P_r , the modulated main flux may couple quite a few magnets to form a complete flux path. It can be clearly seen that the rotor and stator yoke serve as part of this flux path with negligible reluctance.

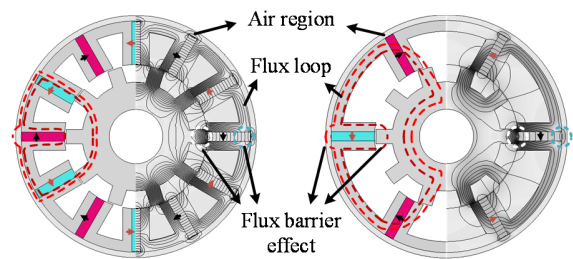


(a) 12/20 stator slot/rotor pole combination. Pole ratio=5:1. (b) 12/22 stator slot/rotor pole combination. Pole ratio=11:1.

Fig. 2. Flux distribution of spoke type VPM machines.

However, when the rotors of surface mounted VPM machines are replaced by spoke type ones, the magnetic circuit of the modulated field becomes quite different. As shown in Fig. 2, when the main flux lines with a small pole number travel into the rotor, they are enforced to bypass the reverse excited magnets into the nearby airgap region. Hence, the amplitude of the modulated magnetic field may be influenced by additional introduced reluctance. The reverse excited magnet can then be regarded as an equivalent flux barrier. Moreover, the larger the pole ratio is, the more flux barriers in the main flux path there will be. Considerable flux barriers may weaken the superiority in torque density for VPM machines.

As another typical FM machine topology, flux switching PM (FSPM) machine is also constructed with spoke-array magnets. Due to the flux modulation effect, there are rich flux harmonics in a FSPM machine with different pole pairs, which can work together to produce fundamental back-EMF and output torque. Fig. 3(a) and (b) illustrate the flux distribution of two typical FSPM machine topologies, with $P_s=4$ and 1, respectively. It can be clearly seen that similar flux barrier effects also exist in FSPM machines. The rotor teeth and yoke can provide flux path with negligible reluctance for the modulated field. Nevertheless, when the working flux harmonics with a relatively small pole pair number of P_s cross the airgap into the stator, they are “hindered” by the reverse excited magnets and “forced” into either the outer air region or the airgap to close the flux loop.



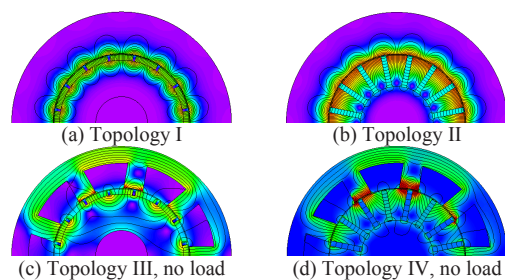
(a) 12/10 stator slot/rotor pole combination. Pole ratio=2.5:1. (b) 6/10 stator slot/rotor pole combination. Pole ratio=10:1.
Fig. 3. Flux distribution of FSPM machines.

III. PERFORMANCE COMPARISON OF NON-SLOTTED AND OPEN-SLOT MACHINE STRUCTURE

In order to further investigate the influence of flux barrier effect on machine performance, quantitative analysis has been conducted on four topologies illustrated in Fig. 4, with special attention on electromagnetic field computation in the airgap. Some fixed parameters are listed in Table I. The PM width of spoke type topologies is ~ 1.3 times that of the surface counterparts to highlight the flux focusing effect.

TABLE I
MAIN DESIGN PARAMETERS OF THE FOUR TOPOLOGIES

| Item | I | II | III | IV |
|---------------------------|---------|-------|---------|-------|
| Outer diameter, mm | 170 | 170 | 170 | 170 |
| Airgap diameter, mm | 105 | 105 | 105 | 105 |
| Airgap length, mm | 1.0 | 1.0 | 1.0 | 1.0 |
| Slot number | - | - | 9 | 9 |
| PM pole pair number | 8 | 8 | 8 | 8 |
| PM type | surface | spoke | surface | spoke |
| PM thickness, mm | 4.0 | 4.0 | 4.0 | 4.0 |
| PM width, mm | 18.6 | 24 | 18.6 | 24 |
| Slot opening ratio | 0 | 0 | 0.6 | 0.6 |
| Turns in series per phase | - | - | 144 | 144 |



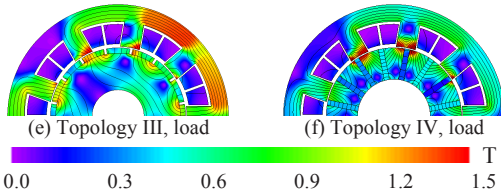


Fig. 4. Flux contour plots of the non-slotted and open-slot topologies.

As shown in Fig. 4(a) and (b), both topology I with surface mounted PMs and topology II with spoke-array PMs are constructed with non-slotted airgap structure. The radial airgap flux density of the two topologies are compared in Fig. 5. It can be seen that the amplitude of 8th flux density produced by the spoke type topology is ~42% larger than that of the surface type one. Hence, the flux focusing effect in topology II has been verified capable of boosting the airgap flux density.

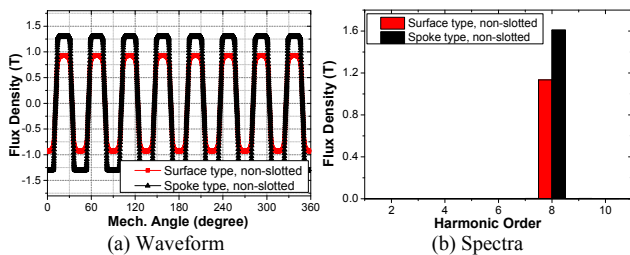


Fig. 5. Airgap flux density comparison between topology I and II.

When the two rotors of topology I and II are combined with the open-slot stator, the resultant no-load airgap flux density comparison is given in Fig. 6. Due to the flux modulation effect, the field harmonic with pole pair number of one is produced. It can be clearly seen from Fig. 6(b) that despite the flux focusing effect, the spoke type topology IV can only produce the 1st harmonic with amplitude 51% that of the surface type counterpart. In summarize, for the specific design of two open-slot topologies with large pole ratio of 8/1, the significant flux barrier effect of the spoke type one has been proved, which results in reduction of the modulated field. Fig. 4(e)-(f) gives the on load flux contour comparison of topology III and IV under 10A phase current ($i_d=0$), with the airgap flux density shown in Fig. 7. It can be seen that the armature reaction of the surface type machine is stronger than that of the spoke type one.

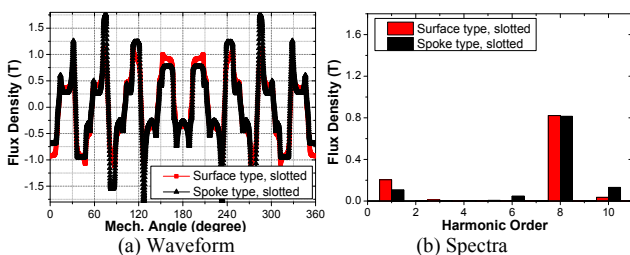


Fig. 6. No load airgap flux density comparison between topology III and IV.

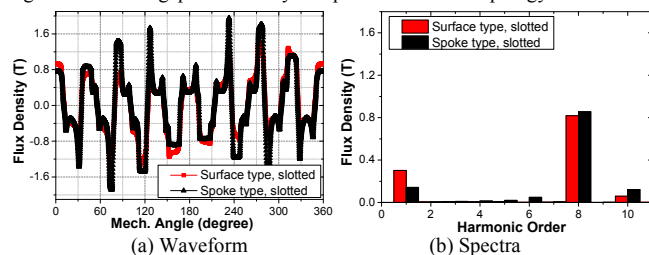


Fig. 7. On load airgap flux density comparison between topology III and IV.

IV. INFLUENCE OF POLE RATIO ON FLUX BARRIER EFFECT

Basically, for FM machines, the larger the pole ratio is, the stronger the flux-modulation effect will be. Therefore, it is necessary to evaluate the variation tendency of flux barrier effect along with pole ratio. In this Section, a series of VPM machine topologies are taken as examples for further investigation, with the main fixed design parameters listed in Table II. It should be noted that for each slot-pole combination, the ratio of spoke type PM width to surface type PM pole arc length is fixed at 1.4/1 for a relatively fair comparison. The flux contour plots of low pole ratio and high pole ratio VPM machines are shown in Fig. 8 and Fig. 9, respectively.

TABLE II
 MAIN DESIGN PARAMETERS OF THE FIVE TOPOLOGIES

| $Z / P_r / P_s$ | 12/8/4 | 18/14/4 | 12/10/2 | 12/11/1 | 18/17/1 |
|---------------------------|--------|---------|---------|---------|---------|
| Outer diameter, mm | 170 | 170 | 170 | 170 | 170 |
| Airgap diameter, mm | 105 | 105 | 105 | 105 | 105 |
| Airgap length, mm | 1.0 | 1.0 | 1.0 | 1.0 | 1.0 |
| Surface PM pole arc | 0.9 | 0.9 | 0.9 | 0.9 | 0.9 |
| Spoke PM width, mm | 26.0 | 14.8 | 20.8 | 18.9 | 12.2 |
| Pole ratio | 2 | 3.5 | 5 | 11 | 17 |
| Turns in series per phase | 192 | 192 | 192 | 192 | 192 |

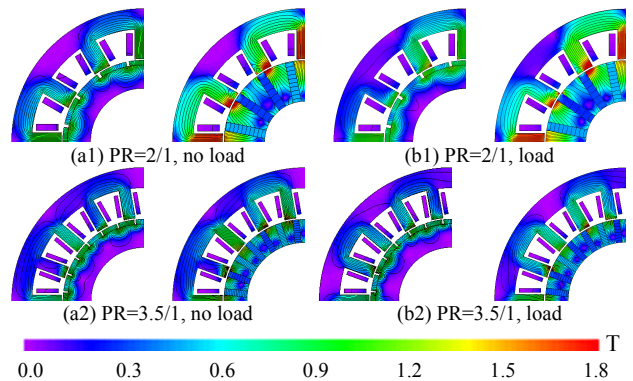


Fig. 8. No load and load flux contour plots of low pole ratio VPM machines with different magnet types.

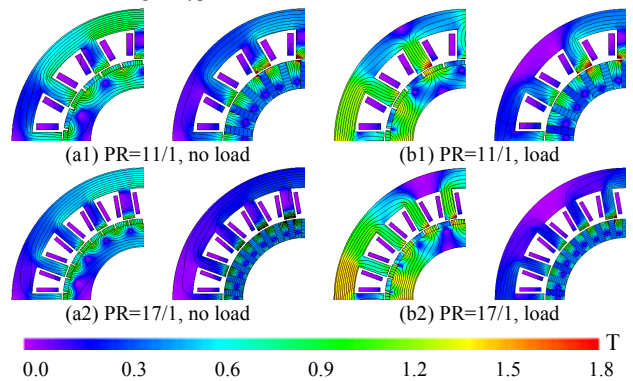


Fig. 9. No load and load flux contour plots of high pole ratio VPM machines with different magnet types.

It can be seen from Fig. 8(a1)-(a2) that for the specific designed VPM machines with relatively low pole ratios, i.e., 2/1 and 3.5/1, the spoke type topologies are with higher no load flux density in the stator yoke than their surface type counterparts, which indicates that the flux barrier effect is weak. However, when PR gets to 11/1 and 17/1 as shown in Fig 9(a1)-(a2), the modulated magnetic field is significantly weakened in the spoke type topology.

In order to further quantify the influence of flux barrier effect on the modulated field, the rightmost term of (5) is rewritten as (6). It should be noted that k_{total} is proportional to the electromagnetic torque when flux leakage and magnetic partial saturation are not considered. k_{conv} and k_{ver} for each topology are then obtained through electromagnetic field computation in the airgap region and illustrated in Fig. 10.

$$k_{conv} = B_{conv}, k_{ver} = \frac{P_r}{P_s} B_{modu}, k_{total} = k_{conv} + k_{ver} \quad (6)$$

It can be seen from Fig. 10 that the influence of flux barrier effect on the modulated part k_{ver} is not obvious in low pole ratio (PR \leq 5) VPM machines. Nevertheless, k_{ver} is significantly reduced in high pole ratio, spoke type VPM machines when compared with the surface type counterparts. Hence, the flux barrier effect may result in serious output torque reduction in such machine topologies. On the other hand, in low pole ratio VPM machines, spoke type PM arrangement is recommended, since both the conventional and vernier part of the electromagnetic torque can be significantly increased.

Fig. 8(b1-b2) and Fig. 9(b1-b2) illustrate the on load flux contour plots of surface and spoke type VPM machines (phase current=10A, $i_d=0$). Seen from the no load and on load plots, it can be found that the armature reaction is getting stronger as PR increases for the surface type VPM machines. Nevertheless, the flux distributions of the on load, spoke type topologies with both low and high pole ratios exhibit no significant variation compared with their no load counterparts. Hence, the armature reaction of the spoke type VPM machine is much weaker than that of the surface type, especially when the pole ratio is high.

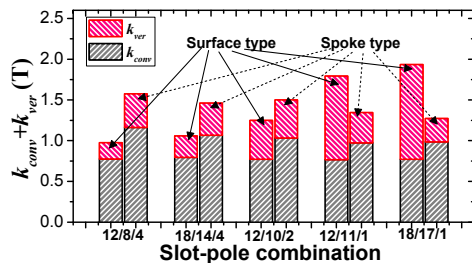
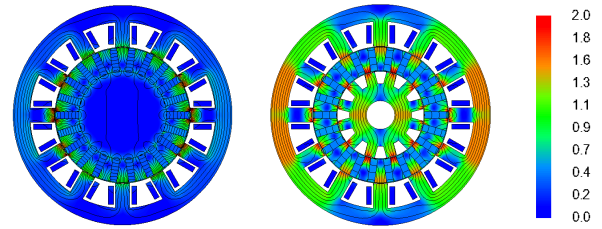


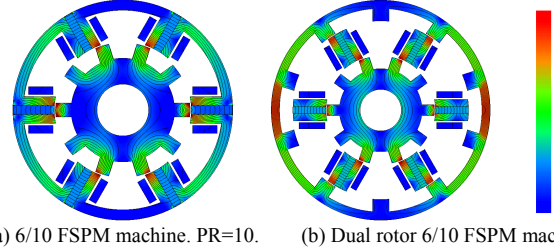
Fig. 10. k_{conv} , k_{ver} and their sum with different magnet types and PRs.

V. DUAL AIRGAP SPOKE TYPE FM MACHINE

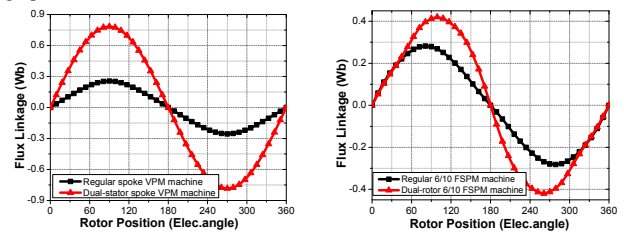
In the forgoing analysis, it has been proven that spoke type VPM machine with a high pole ratio may not be a cost-effective option due to significant flux barrier effect. In fact, if extra flux path with negligible reluctance could be provided for the modulated magnetic field, the flux barrier effect could be avoided. In the already proposed dual stator spoke type VPM machine [6] and dual rotor FSPM machine [5], the dual stator/dual rotor topology exactly provides this additional flux path for each other, as shown in Fig. 11 and Fig. 12. The dual side, spoke type topologies were first proposed to improve the power factor and torque density, while it should be noted that the topologies in Fig. 11(b) and Fig. 12(b) share exactly the same working principle. It can be seen from the Fig. 13 that the induced flux linkage of the dual side topologies are much larger than those of the regular counterparts, which can in turn verify the effectiveness of these two topologies.



(a) Regular type. PR=11 (b) Dual stator type. PR=11.
Fig. 11. Flux contour plots of regular and dual stator spoke type VPM machine.



(a) 6/10 FSPM machine. PR=10. (b) Dual rotor 6/10 FSPM machine.
Fig. 12. Flux density comparison of regular and dual rotor FSPM machine with high pole ratio.



(a) VPM machine, PR=11 (Outer stator). (b) FSPM machine, PR=10.
Fig. 13. Flux linkage comparison of regular and dual side, spoke type FM machines with high pole ratio.

VI. CONCLUSION

This paper provides the performance comparison of surface and spoke type flux-modulation machines from the perspective of flux density distribution. Through the comparison, a flux barrier effect in spoke type flux-modulation machines has been found and analyzed in detail. Through numerical FEA on both no load and load condition, the flux barrier effect has been proven capable of weakening the modulated magnetic field and output torque when the machine is equipped with a high pole ratio.

REFERENCES

- [1] D. Li, R. Qu, J. Li, "Topologies and analysis of flux-modulation machines," In *Energy Conversion Congress and Exposition (ECCE)*, Montreal, Canada, 2015, pp. 2153-2160.
- [2] Q. Chen, G. Liu, W. Zhao, M. Shao, "Nonlinear Adaptive Lumped Parameter Magnetic Circuit Analysis for Spoke-Type Fault-Tolerant Permanent-Magnet Motors," *IEEE Trans. Magn.*, vol. 49, no. 9, pp. 5150-5157, Mar. 2013.
- [3] F. Li, W. Hua, M. Tong, G. Zhao, and M. Cheng, "Nine-phase flux-switching permanent magnet brushless machine for low-speed and high-torque applications," *IEEE Trans. Magn.*, vol. 51, no. 3, pp. 8700204, Mar. 2015.
- [4] X. Li, K. T. Chau, M. Cheng, B. Kim, and R. D. Lorenz, "Performance analysis of a flux-concentrating field-modulated permanent-magnet machine for direct-drive applications," *IEEE Trans. Magn.*, vol. 51, no. 5, pp. 8104911, May. 2015.
- [5] B. Zhang, M. Cheng, J. Wang, and S. Zhu, "Optimization and Analysis of a Yokeless Linear Flux-Switching Permanent Magnet Machine with High Thrust Density," *IEEE Trans. Magn.*, accepted.
- [6] B. Kim, T. Lipo, "Analysis of a PM Vernier Motor With Spoke Structure," *IEEE Trans. Ind. Appl.*, vol. 52, no. 1, pp. 217-225, Sep. 2016.